Peptide Nucleic Acids as miRNA Target Protectors for the Treatment of Cystic Fibrosis

Federica Zarrilli [1,2], Felice Amato [2,3], Carmine M. Morgillo [4], Brunella Pinto [4], Giuliano Santarpia [4], Nicola Borbone [4], Stefano D'Errico [4], Bruno Catalanotti [4], Gennaro Piccialli [4], Giuseppe Castaldo [2,3] and Giorgia Oliviero [3,*]

[1] Department of Biosciences and Territory, University of Molise, Isernia, Italy
[2] CEINGE – Advanced Biotechnologies Scarl, Napoli, Italy
[3] Department of Molecular Medicine and Medical Biotechnologies, University of Naples Federico II, Napoli, Italy
[4] Department of Pharmacy, University of Naples Federico II, Napoli, Italy
* Correspondence: golivier@unina.it; Tel.: +39-081-679-896

Text S1: Correlation between torsion angles in the PNA strands.

The analysis of PNA torsion angles performed with Curves + showed a high degree of deviation and flexibility, and particularly pronounced in the case of α and ε torsion angles. Indeed, in all MD simulations, two main average values were found, for α (-100 ° and 100 °) and ε (-20 ° and 180 °) (Figure S2). The analysis of distribution of torsion angles revealed that in our simulation 80% of values ranged around -100 °, in both **1**/RNA and **2**/RNA heteroduplexes, while ε assumed preferentially values around 180 °(Figure S1). To check whether the discrete values assumed by these torsion angles were correlated, the Pearson correlation coefficient was calculated on the torsion angle ε of the residue i and the torsion $\alpha_{(i+1)}$ of the subsequent base, sampled on 0.1 ns interval. Indeed, it has been previously reported that these angles were correlated in PNA containing duplexes [S-1].

The results, reported in Table S5, showed that for both **1**/RNA and **2**/RNA heteroduplexes the Pearson correlation coefficients between ε_i and $\alpha_{(i+1)}$ are all below 0.3, suggesting the lack of consistent correlation.

To further explore structural features of PNA/RNA heteroduplexes, was also analysed the correlation between the pseudo torsion ν_i and the torsion angle α of the subsequent base. The torsion angle ν, defined as the angle between C8´-N4´-C´-O1´ (Main text, Figure 8, red circles), has been proposed as a pointer of the orientation of the backbone carbonyl with respect to the strand terminus [S-2]. The high Pearson correlation coefficients calculated revealed that there is a strong anti-correlation between the pseudo torsion angle ν_i and $\alpha_{(i+1)}$ of the subsequent base (Main text, Table 3).

The correlation found between negative values of $\alpha_{(i+1)}$ and positive values of ν_i in both **1**/RNA and **2**/RNA duplexes determines the orientation of the backbone carbonyl towards the N-terminus. Accordingly, the measure of the distance between the two carbonyl oxygens in each PNA base resulted in the range 3.4 Å - 4.1 Å, in good agreement with previously reported data [S-2].

References

S-1. He, W.; Hatcher, E.; Balaeff, A.; Beratan, D.N.; Gil, R.R.; Madrid, M.; Achim, C. Solution structure of a peptide nucleic acid duplex from NMR data: features and limitations. *J. Am. Chem. Soc.* **2008**, 130(40), 13264-13273.

S-2. Soliva, R.; Sherer, E.; Luque, F.J.; Laughton, C.A.; Orozco, M. Molecular dynamics simulations of PNA–DNA and PNA–RNA duplexes in aqueous solution. *J. Am. Chem. Soc.* **2000**, *122(25)*, 5997–6008.

Table S1. Heteroduplexes systems modelled and analysed by MD simulations. The tetrapeptide tail at PNA C-end is reported in italics characters.

PNA **1** /RNA	G_1-A_2-A_3-G_4-A_5-A_6-G_7-C_8-A_9-C_{10}-C_{11}-A_{12}-A_{13}-U_{14}-C_{15}-A_{16}-U_{17}-G_{18}-A_{19} | | | | | | | | | | | | | | | | | | | *G_{36}-S (P) $_{35}$-S (P) $_{34}$-G_{33}*-**c_{32}-t_{31}-t_{30}-c_{29}-g_{28}-t_{27}-g_{26}-g_{25}-t_{24}-t_{23}-a_{22}-g_{21}-t_{20}**
PNA **2** /RNA	G_1-C_2-A_3-C_4-C_5-A_6-A_7-U_8-C_9-A_{10}-U_{11}-G_{12}-A_{13} | | | | | | | | | | | | | | *G_{36}-S (P) $_{35}$-S (P) $_{34}$-G_{33}*-**-g_{20}-g_{19}-t_{18}-t_{17}-a_{16}-g_{15}-t_{14}**

Table S2. Output of the hierarchical clusterization performed with Ambertools 15 using a RMS metric comparing the heavy atoms in the central duplex base-pairs. Only clusters with population higher than 0.1% were reported.

#Run1 PNA **1**

#Cluster	Frames	Frac	AvgDist	Stdev	Centroid	AvgCDist
0	2315	0.772	1.941	0.518	1285	3.029
1	481	0.160	1.947	0.551	2693	3.085
2	127	0.042	1.862	0.485	1748	2.916
3	74	0.025	1.788	0.388	1473	3.783
4	2	0.001	2.385	0.000	2355	3.798

#Run2 PNA **1**

#Cluster	Frames	Frac	AvgDist	Stdev	Centroid	AvgCDist
0	6263	0.973	1.881	0.557	3612	2.836
1	171	0.027	1.871	0.557	5365	3.676

#Run3 PNA **1**

#Cluster	Frames	Frac	AvgDist	Stdev	Centroid	AvgCDist
0	408	0.816	3.498	0.828	207	5.008
1	49	0.098	3.407	0.740	161	4.975
2	37	0.074	3.555	0.773	143	5.312
3	5	0.010	3.327	0.808	167	5.616
4	1	0.002	0.000	0.000	444	6.192

#Run1 PNA **2**

#Cluster	Frames	Frac	AvgDist	Stdev	Centroid	AvgCDist
0	3063	0.974	1.099	0.237	96	1.538
1	31	0.010	1.062	0.207	1431	1.796
2	29	0.009	1.246	0.226	2317	1.937
3	20	0.006	1.211	0.251	246	1.676

#Run2 PNA **2**

#Cluster	Frames	Frac	AvgDist	Stdev	Centroid	AvgCDist
0	2937	0.987	1.144	0.243	1030	1.739
1	29	0.010	1.221	0.256	884	1.889
2	5	0.002	1.205	0.157	1409	1.906
3	3	0.001	1.385	0.284	1044	1.996
4	3	0.001	1.283	0.328	1248	1.898

#Run3 PNA **2**

#Cluster	Frames	Frac	AvgDist	Stdev	Centroid	AvgCDist
0	2991	0.997	1.198	0.263	1163	1.802
1	5	0.002	1.543	0.271	2172	1.967
2	2	0.001	0.933	0.000	2143	1.996

Table S3. RMSD in Å between the average structures of clusters with population higher than 5% obtained from the MD simulation of **1**/RNA heteroduplex.

#Cluster	run2_0	run3_0
run1_0	0.118	0.234
run2_0	-	0.242

Table S4: RMSD in Å between the average structures of clusters with population higher than 5% obtained from the MD simulation of **2**/RNA heteroduplex.

#Cluster	run1_1	run2_0	run3_0	run3_1	run3_2
run1_0	2.207	0.305	0.216	1.902	1.793
run1_1	-	2.268	2.240	1.504	2.880
run2_0	-	-	0.196	1.806	1.703
run3_0	-	-	-	1.893	1.797
run3_1	-	-	-	-	2.013

Table S5: Pearson correlation coefficients between torsion angles ε_i and $\alpha_{(i+1)}$ and between the pseudo torsion angle ν_i and the torsion angle $\alpha_{(i+1)}$. Indexes were calculated on the central bases of **1**/RNA or **2**/RNA heteroduplexes, on the basis of 0.1 ns sampling of torsion angles. Definition of torsion angles is given in Main text, Figure 8.

		Pearson ε_i:$\alpha_{(i+1)}$			Pearson ν_i:$\alpha_{(i+1)}$		
1		Run1	Run2	Run3	Run1	Run2	Run3
	g_{21}	-0.01	-0.17	-0.24	-0.48	-0.68	-0.76
	a_{22}	0.05	0.03	0.04	-0.42	-0.45	-0.43
	t_{23}	-0.30	-0.31	-0.28	-0.79	-0.80	-0.79
	t_{24}	-0.27	-0.20	-0.30	-0.78	-0.79	-0.82
	g_{25}	-0.26	-0.18	-0.18	-0.81	-0.76	-0.75
	g_{26}	-0.24	-0.17	-0.15	-0.74	-0.68	-0.69
	t_{27}	-0.27	-0.28	-0.30	-0.81	-0.79	-0.83
	g_{28}	-0.29	-0.22	-0.23	-0.79	-0.79	-0.78
	c_{29}	-0.16	-0.10	-0.10	-0.71	-0.68	-0.61
	t_{30}	-0.24	-0.26	-0.19	-0.81	-0.81	-0.78
2							
	g_{15}	-0.21	-0.32	-0.16	-0.69	-0.85	-0.78
	a_{16}	0.03	0.01	-0.02	-0.56	-0.49	-0.52
	t_{17}	-0.37	-0.35	-0.37	-0.84	-0.82	-0.85
	t_{18}	-0.17	-0.23	-0.20	-0.68	-0.76	-0.69

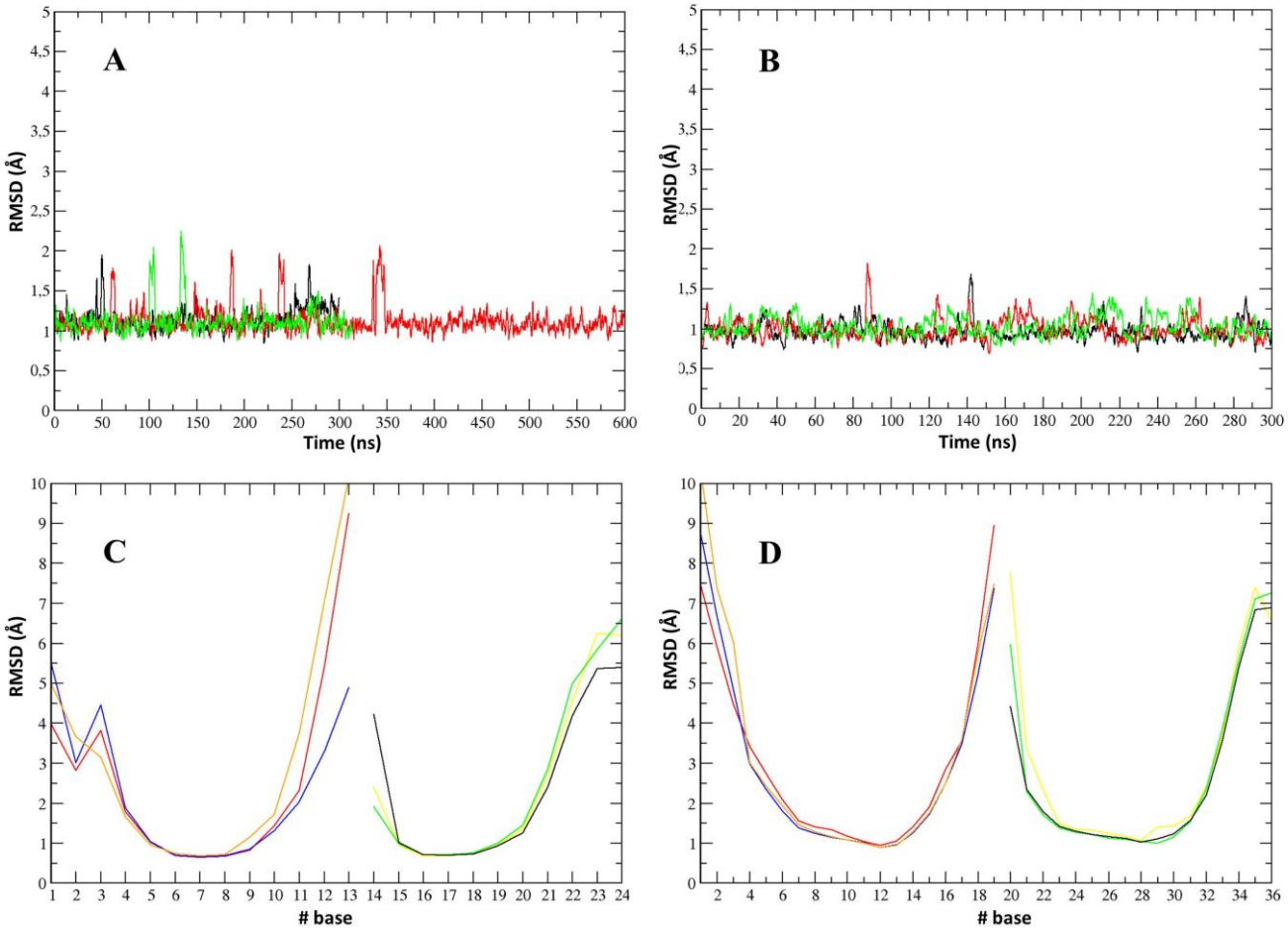

Figure S1. Up: Root-mean-square deviation versus time in the three MD runs on **2**/RNA (A) and **1**/RNA (B). Superpositions were made on the central base-pairs using thermalized structures as reference. Down: Root-mean-square fluctuations in the three MD runs on **2**/RNA (C) and **1**/RNA (D) where the X-axis represents the residue numbering in the sequence (see Table S1 for residue numbering). Colour codes: PNA strand run 1: yellow; RNA strand run 1: red; PNA strand run 2: green; RNA strand run 2: blue; PNA strand run 3: black; RNA strand run 3: orange.

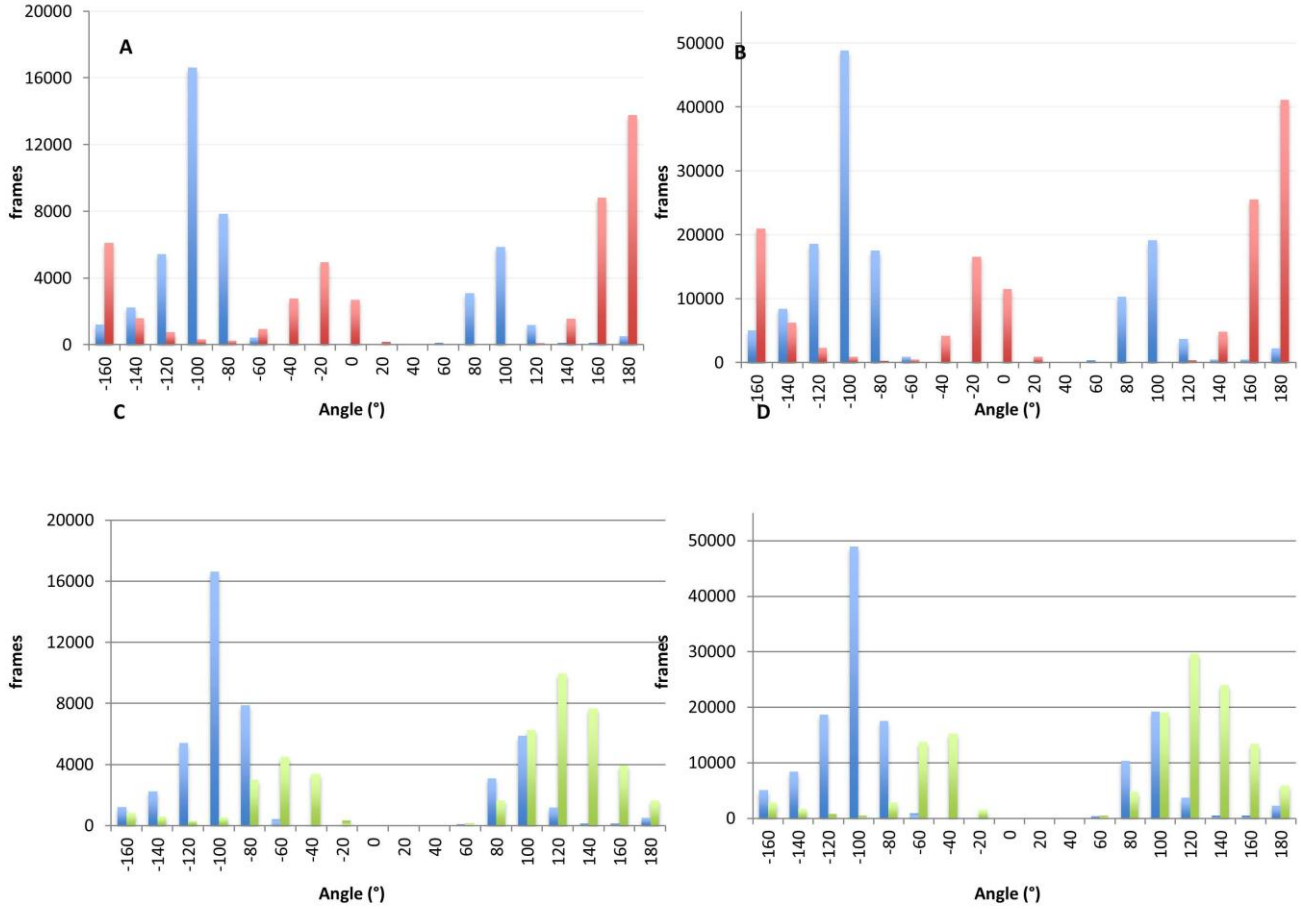

Figure S2. Distribution of the torsion angles α (blue) and ε (red) and the pseudo torsion angle ν (green) of PNA strand during the MD run of **2** (A and C) and **1** (B and D) heteroduplexes. Angles were sampled every 0.01 ns.